Initial Studies of Array Feeds for the 70-Meter Antenna at 32 GHz

P. W. Cramer
Ground Antennas and Facilities Engineering Section

The results of a study to determine the feasibility of using array feed techniques to improve the performance of the 70-m antenna at 32 GHz are presented. Changing from 8.4 GHz to 32 GHz has the potential of increasing the gain by 11.6 dB, but recent measurements indicate that additional losses of from 3 to 7 dB occur at 32 GHz, depending on the elevation angle. Array feeds have been proposed to recover some of the losses by compensating for surface distortions that contribute to these losses. Results for both surface distortion compensation and pointing error correction are discussed. These initial studies, however, had one significant restriction: The mechanical finite-element model was used to characterize the surface distortions, not the measured distortions from three-angle holography data, which would be more representative of the actual antenna. Further work is required to provide for a more accurate estimate of performance that utilizes holography data and, in particular, one that evaluates the performance in the focal plane region of the antenna.

I. Introduction

To achieve a significant performance improvement from the Deep Space Network (DSN), it has been proposed that the operating frequency be increased to 32 GHz. Currently the maximum operating frequency for the 70-m antennas is 8.4 GHz, and these ground antennas were designed to operate efficiently up to this frequency. Assuming that both the spacecraft and ground antennas have the same efficiencies at both frequencies, a performance improvement of 11.6 dB could be expected by changing to 32 GHz. However, measurements performed on the 70-m antenna by Gatti [1] at 32 GHz indicated that losses of 4.6 dB were observed at the rigging angle. The rigging angle is the antenna elevation angle at which the antenna surface shape has been adjusted to minimize losses. Compared to 1.5 dB at 8.4 GHz [2], this represents a reduction in potential performance by 3.1 dB at the rigging angle.

The 32-GHz measurements also indicated that at an elevation angle of 15 deg the losses were 8.8 dB, an increase of 4.2 dB over the 4.6 dB measured at the rigging angle. At 8.4 GHz the increase in losses over the range of operating elevation angles is under 0.3 dB. The additional losses measured at 32 GHz are a significant part of the potential performance improvement that is to be gained by going to the higher frequency and must be recovered if moving to the higher frequency is to be justified. The work covered by this article analyzes one method that has been proposed to recover a portion of these losses.

Some of these losses are a function of the antenna elevation angle and are due to gravitationally induced reflector surface errors. The surface errors cause distortions in the antenna focal plane field distributions, which are not coupled efficiently into the antenna feed. It has been proposed that an array feed be used to sample the distorted focal plane fields. By proper weighting of the contributions from each array element, the lost performance could then be recovered. This concept would be directed toward recovering a significant portion of the 4.2-dB gravitationally induced surface distortion loss.

A second problem of operating at 32 GHz is the reduction in the antenna pattern beamwidth. The one-sigma pointing accuracy of the 70-m antenna is presently on the order of 0.003 deg. At 32 GHz a pointing error of this magnitude can produce a loss of 1.75 dB. Again, the use of an array feed has been proposed to recover the pointing losses. Blank and Imbriale [3] have analyzed the case for an array feed used with a single distorted parabolic reflector, presenting results covering both distortion compensation and correction for pointing errors. This article extends this work to cover dual-shaped reflector antennas typical of the 70-m antennas used in the DSN.

II. Analytical Approach

The antenna that is the subject of this study is the 70-m antenna at DSS 14 (Fig. 1). The antenna has optimally shaped reflector surfaces to maximize efficiency. The actual antenna has an offset feed horn and an asymmetric subreflector design to facilitate horn switching. However, to simplify the study, only a non-offset symmetrical geometry was analyzed. Figure 2 shows the layout of the feed horn array, which is located in the focal plane of the antenna. The horns are positioned in a triangular lattice consisting of four rings of elements, the outer boundaries of each ring being hexagonal in shape. This allows the analysis to evaluate different-sized arrays: using one ring with one element, two rings with seven elements, three rings with 19 elements, and four rings with 37 elements. The coordinate system convention used is that the z axis is along the direction in which the antenna is pointed and the elevation axis is normal to the plane containing the y and z axes, with positive y pointing upward.

To determine the maximum performance that can be achieved with an optimally excited array-fed antenna system, the conjugate weighting method is used [3], as described in the following procedure. The antenna system far field at a common observation point is calculated for each horn in the array feed. Next, each feed horn excitation is set equal to the conjugate value of the corresponding far-field value at the common observation point. This in effect weights each far-field point by its complex conjugate. Then the weighted far-field values are summed and normalized, as given by

$$G_m = \frac{4\pi \left(\sum_{K=1}^{N} |E_K|^2 \right)^2}{\eta P_t} \tag{1}$$

and

$$P_t = \frac{1}{\eta} \int_o^{2\pi} \int_o^{\frac{\pi}{2}} |f(\theta,\phi) \sum_{K=1}^{N} E_K^* \, e^{jk\hat{R} \cdot \bar{r}_K}|^2 \sin\theta \, d\theta \, d\phi \tag{2}$$

where

E_K = the antenna complex far-field vector associated with the Kth horn

k = wave number

$f(\theta,\phi)$ = field pattern of array horn (assumes no mutual coupling)

$\bar{r}_K$ = array horn position vector in focal plane

$\hat{R}$ = unit vector in direction of observation point

θ,ϕ = spherical coordinates of observation point

N = number of horns in array feed

η = free-space impedance

with G being an estimate of the performance that can be expected from an antenna with distorted surfaces using an array feed to compensate for the errors. To simplify the calculation and to get the best estimate, the direction of the observation point was selected to be in the direction of the pattern peak when only the center element is used.

A finite-element mechanical model [4], identified as model J, is used to describe the antenna geometry and surface shape that results from gravity loading of the antenna at the various elevation angles considered. The errors in the surface shape and antenna geometry were supplied to this task in the form of y-gravity and z-gravity load-interpolating coefficients, independent of the elevation angle. To determine the errors at a given elevation angle, the following generic interpolating function is used:

$$P = P_z[\sin(rig) - \sin(elev)] + P_y[\cos(rig) - \cos(elev)] + const \tag{3}$$

where *rig* is the rigging angle and *elev* is the elevation angle of interest, P_z and P_y are z and y gravity coefficients, and *const* allows the use of a constant term where an error term is not zero at the rigging angle. Each antenna error, such as a subreflector displacement or movement of a reflector surface point, is described by a three-component-vector set of P_z and P_y. Using the above expression, the three vector components of a given error P can be calculated as a function of elevation angle. The mechanical model used assumes that the gravity-induced errors or distortions are symmetrical with respect to the vertical axis (y axis). Therefore, there are no coefficients for subreflector displacements or antenna beam boresight movements in the x direction.

The finite-element mechanical model defines the distorted reflector shape in terms of a vector $\mathbf{V}(u, v, w)$, which defines a point on the distorted surface relative to a corresponding reference point on a perfect reflector. The antenna pattern analysis program requires that the surface errors be defined by an axial or z-directed displacement relative to a perfect reflector surface. Figure 3 illustrates the method used to derive the axial term. The vector $\mathbf{V}(u, v, w)$ is defined relative to the point (X_0, Y_0, Z_0) on the undistorted main reflector surface. The values of X_0 and Y_0 are used to calculate Z_0, in this case on the surface of a shaped main reflector. This point, along with vector $\mathbf{V}(u, v, w)$, defines a point on the distorted surface (X_1, Y_1, Z_1). The value of Z_2 is calculated on the surface of the shaped main reflector at (X_1, Y_1). The difference, $D_z(z)$, between points (X_1, Y_1, Z_1) and (X_1, Y_1, Z_2) defines the axial surface error term.

Since the analysis program needs the distorted surface defined at points other than those in the table of $(X_1, Y_1, D_z(z))$, an interpolation function is required. A local interpolating scheme recommended in [5] was selected. The surface of the reflector is subdivided into a number of regions approximately equal to the number of surface panels used on the 70-m antenna. A two-dimensional quadratic function is then best-fitted with up to 16 points from the error table, the points selected being closest to the center of the interpolating region. Fewer than 16 points might be used if the program determines that some of the points are too remote from a given region. The surface error interpolating function is of the form

$$D_z = a_1 + a_2 x + a_3 y + a_4 x^2 + a_5 xy + a_6 y^2 \qquad (4)$$

The procedure used in the analysis is shown in Fig. 4. The gravity load interpolating coefficient table for the reflector, supplied by R. Levy, is the input for the DIST-RAW program, which computes the actual surface distortions for a given elevation angle. The output of the DIST-RAW program is entered into the DIST-COE program to compute the two-dimensional local interpolating coefficients in Eq. (4) that define the surface errors for the scattering calculation program. A second set of gravity load interpolation coefficients, describing the motion of the subreflector and the antenna beam boresight location, is entered into the RUNGEN program, which calculates the subreflector and boresight location for the specified elevation angle, then calculates the geometry between the reflector surfaces and the array feeds, and finally generates a run stream for calculating the antenna system far-field pattern for each of the array feeds. The horn patterns, the table of data for the undistorted surfaces, and the output of the DIST-COE and RUNGEN programs are entered into the scattering program, and the scattering program is run once for each of the array feed horns. The GTD/Jacobi-Bessel scattering program is used. The output of each run of the scattering program, along with the horn pattern, is entered into the GAIN-EFF program, which evaluates Eqs. (1) and (2).

III. Optimum Antenna Configuration

To achieve the most improvement and maximize the effectiveness of the array feed in compensating for surface distortions, the subreflector position was adjusted analytically to provide maximum gain at two representative antenna elevation angles, using the calculated pattern for a single standard 22-dB horn. (This capability currently exists, where the DSN antenna subreflectors are moved to compensate for gravity-induced deflections, using a simple elevation-dependent algorithm.) Adjustments were made both vertically and along the antenna axis. At each subreflector position, the gain was calculated in the direction of the predicted boresight angle associated with the selected elevation angle. Using the subreflector adjustments for elevation angles of 15 and 75 deg, a set of gravity coefficients for the Levy interpolation function was derived:

For z-axis movements	$P_y = \ \ 0.041850$ in.
	$P_z = -0.941735$ in.
For y-axis movements	$P_y = -2.579083$ in.
	$P_z = -0.545444$ in.

The best boresight location was found to be very close to those predicted by Levy's model J, and therefore his interpolation function coefficients are used for the boresight predictions. The coefficients used are:

Main reflector rotation about x axis	P_y =	−1852.8 sec
	P_z =	0.3 sec
Main reflector translation in y direction	P_y =	1332.7 sec
	P_z =	7.0 sec

The effect of the subreflector translation on the antenna boresight location is not defined in terms of gravity interpolation coefficients. Instead, the following expression supplied by Levy is used:

$$B = 0.0374\ Y_t \text{ deg/in. about } x \text{ axis} \qquad (5)$$

where Y_t is the total subreflector motion in the y direction and B is the boresight shift contribution due to the subreflector.

In the analysis that follows, it is assumed that the surface errors are strictly due to time-invariant distortions caused by gravitational loads. Any losses due to small-scale surface errors are not accounted for, since these errors are not predicted by the mechanical model. Even if the small-scale surface errors could be predicted, they would not be included because this would require an array with a very large number of unrealizably small elements. In measurements made on the 70-m antenna at 32 GHz and at a rigging angle of 45.5 deg [1], an efficiency of 35 percent was observed for a loss of 4.56 dB. At 8.4 GHz and at an elevation angle of 45 deg, there is a blockage loss of 0.45 dB [2]. If it is assumed that this loss is also typical of the performance at 32 GHz and the calculated directivity efficiency at 45 deg is 0.37 dB, then, subtracting these losses from 4.56 dB, a loss of 3.74 dB remains. Since the efficiency was measured while the antenna was at the rigging angle, where the surface is adjusted to remove any systematic surface errors, it could be assumed that the 3.74-dB loss is due to random small-scale errors in the individual panels. A small-scale error loss of 3.74 dB is equivalent to about a 0.7-mm root mean square (rms) surface error using Ruze's analysis.

Microwave holography imaging at 12 GHz shows all DSN 70-m antennas, in their initial (1988) state of adjustment, as having approximately a 0.7-mm rms error at the rigging angle. Therefore, the assumption that the 3.74-dB loss is a small-scale error loss is reasonable. Since it is not likely that an array feed would be able to compensate for this type of loss, there may be a loss in excess of 3.0 dB which is not recoverable using array techniques. Because the study assumes a model that includes only gravitational loads, this loss does not show up in the following analysis. If the overall loss is needed, then 4.19 dB (4.56−0.37 dB) needs to be added to the losses or efficiencies presented in this article. In other words, the analysis considered here will not significantly improve the antenna efficiency at the rigging angle, which is about 35 percent as measured in [1]. It should be noted that evidence exists that the 0.7-mm rms small-scale surface errors can be reduced to 0.45 mm by means of a more time-consuming panel adjustment. This procedure might increase the efficiency to approximately 50 percent at the rigging angle.

A. Effects of Element Size on Performance

Once the best geometry is established, the next step is to determine the effect of the array feed horn element size on the ability of the array to recover lost efficiency. Since the geometry selected places the array elements on a triangular lattice, the element size establishes the element spacing. Four array sizes were evaluated: 1, 7, 19, and 37 elements. An extreme antenna elevation angle of 75 deg was selected for calculation. The results for element diameters ranging from 0.25 in. (0.68 wavelength) to 2.00 in. (5.4 wavelengths) are shown in Fig. 5 for zero-thickness walls. Figure 6 is a similar plot for a smaller range of horn sizes, for horns with 0.05-in.-thick walls. The 0.25-in. diameter is the smallest practical size to be considered, since the cutoff diameter for the TE_{11} fundamental mode at 32 GHz is 0.216 in. At a diameter of 0.5 in., the TM_{11} mode can be supported. Therefore, single-mode horns were evaluated for diameters less than 0.5 in., and dual-mode horns were evaluated for diameters of 0.5 in. and larger. Because dual-mode horns equivalent to the 22-dB standard hybrid-mode horns have aperture sizes of about 1.75 in., this size was included as the largest practical size of interest, and the plot was extended to 2.00 in. to see how the curve behaved beyond the largest practical size.

The curve for a single element is what one would expect (Fig. 5). The gain peaks at about 1.75 to 2.00 in., where the best performance would normally be found if no distortions were present, since the antenna optical design was optimized for horns of this size. As the element size becomes smaller, the efficiency drops, as expected, since the antenna reflectors become overilluminated. Looking at the curves for more elements, it can be seen that the additional elements do not compensate for the illumination losses until a diameter of 0.75 in. is reached, and then the performance is still not as good as at 1.75 in. or above. It is not until the single-mode conical horn size of 0.35 in. is reached and 19 or more elements are used that performance equivalent to the larger dual-mode horns is approached. Thus the performance reaches a maximum for horn diameters of approximately 0.35 and 1.75 in.

For a more detailed study, the cases of interest are those with 1.75- and 0.35-in.-diameter horns. To answer the question of whether an intermediate point might be better if pointing or subreflector errors are considered, the 1.25-in. case was also selected. Finally, a case using the standard 22-dB corrugated (hybrid-mode) horns was selected as a reference case. The spacing for the corrugated horns is 2.2 in. to allow space for the corrugations.

The horn wall thickness affects how closely the horns can be positioned. If the horn walls are tapered at the aperture, then they can be spaced as if there were no wall thickness. This is the case in Fig. 5. To illustrate the effect of wall thickness, a set of calculations for horns with 0.05-in. walls at the aperture was made, and the results are plotted in Fig. 6. The efficiency for a series of horns with 0.05-in.-thick walls falls off more rapidly than for zero thickness simply because the horn size refers to the maximum horn diameter and the wall thickness then detracts from the horn's effective aperture. The effect is more pronounced for the smaller sizes, since the wall thickness accounts for a larger percentage of the horn size. For all arrays with elements smaller than 1.75 in., zero wall thickness gives significantly better results. For 1.0-in.-diameter elements, for example, the differences are on the order of 1.0 dB. This is one illustration of how critical the feed design is to achieving the maximum recovery of the energy in the antenna focal region.

B. Effects of Antenna Elevation Angle

Figures 7 through 10 show the performance of the array feed as a function of the antenna elevation angle. (Note the change in the range of elevation angles in Fig. 8.) It can be seen that the performance peaks at 45 deg and then drops off as the elevation angle either increases or decreases. The best performance is obtained at 45 deg because the antenna surface shape is adjusted at this angle to compensate for any gravitational distortions. This is referred to as the rigging angle. The rigging angle could be any angle, but for the structural model used in this study the angle was set at 45 deg. As the antenna elevation angle diverges from the rigging angle, further gravitational errors cause the surface to deviate from the optimum shape and the antenna efficiency begins to degrade. With the exception of the case shown in Fig. 8, the elevation angles for this study range from 7.5 to 75 deg, which covers the operational angles imposed on the antenna system.

The effects of element spacing can be seen by comparing the curves for the standard hybrid-mode horn (2.2-in. diameter) in Fig. 7 and the 1.75-in. dual-mode horn in Fig. 8. For the single-element case the performance is the same for both horn types to within a few hundredths of a decibel over the range of elevation angles. This is to be expected, since the patterns for a single horn for these two cases are very similar. The efficiency ranges from −3.5 through −0.4 to −2.3 dB over these elevation angles, showing that there is significant room for improvement. When seven elements are used, the dual-mode horns with their denser packing have better performance by 0.5 dB at 7.5 deg than the hybrid-mode horns. With 37 elements, the difference at 7.5 deg is 0.6 dB, and at 75 deg it is 0.13 dB.

Considering the 1.75-in. dual-mode configuration only, the following observations can be made. At 45 deg, the loss is 0.42 dB for a single horn, which is the directivity loss for an undistorted reflector; with a properly designed feed such as the one used, it represents the best performance achievable. Using additional horns at 45 deg does not change the performance. At an elevation angle of 7.5 deg, a single element has a loss of 3.48 dB, seven elements have a loss of 2.04 dB, and 37 elements have a loss of 1.72 dB. Thus there is an improvement of 1.44 dB when going from one to seven elements and 1.77 dB when going to 37 elements. At an elevation angle of 75 deg, a single element has a loss of 2.35 dB, seven elements have a loss of 1.73 dB, and 37 elements have a loss of 1.49 dB. In this case there is an improvement of 0.62 dB when going from one to seven elements and 0.85 dB when going to 37 elements. The array feed in effect has halved the losses due to surface distortion when using 37 elements at the extremes in elevation angles, with most of the improvement achieved by adding one ring of elements for a total of seven elements.

The performance curves shown in Fig. 9 for the 1.25-in. dual-mode horns are considerably lower than those for the previous cases at all elevation angles and for any number of horns. The loss at 45 deg with a single element is 1.33 dB because the antenna is overilluminated by the smaller horn. It is interesting to note, however, that with additional elements at this elevation angle no significant performance improvement is achieved. This shows that, for shaped-reflector designs and with small reductions in horn size, the outer horns do not effectively capture the small amount of energy no longer collected by the center element. For the 0.35-in. single-mode horn (Fig. 10), it takes 19 elements to get to within 0.0 to 0.2 dB of a single 1.75-in. horn over the range of elevation angles calculated. It takes 37 elements to get within 0.1 dB of a single 1.75-in. horn at a 45-deg elevation angle. Thus, for cases where the antenna is properly pointed and the subreflector is in the optimum position for the elevation angle, the smaller elements provide no real advantage and the 1.75-in. dual-mode horn is the better choice.

C. Performance Versus Pointing Angle

In addition to compensating for distortions with a properly pointed antenna, an array feed can also be used to correct for antenna pointing errors. These pointing errors can be due to rapid changes in the surface distortion, a lack of knowledge of what the pointing errors are for a given elevation angle, or a limitation in the pointing accuracy of the antenna control system. A pointing accuracy on the order of 0.003 deg is considered good for the 70-m antenna and causes a negligible loss at 8.4 GHz, the current maximum operating frequency. At 32 GHz, however, a pointing error of this magnitude can give rise to a 1.75-dB loss. Pointing errors were simulated in this study by calculating the performance improvements along directions at various angles relative to the best antenna pointing angle (boresight). With one exception, the calculations were made at an elevation angle of 75 deg so as to include the effects of surface distortions. Cases were calculated for 0.35-in. single-mode horns, for 1.25- and 1.75-in. dual-mode horns, and for a 2.2-in. hybrid-mode horn. The one exception is the 2.2-in. hybrid-mode horn, for which an elevation angle of 45 deg was used.

The performance of the 2.2-in. hybrid-mode horn is shown in Figs. 11 and 12. For an elevation angle of 45 deg (Fig. 11), it can be seen that the performance as a function of boresight offset angle is virtually the same for any number of elements. This indicates that only one element is contributing to the antenna performance. Figure 13 illustrates the antenna beam patterns for four feed elements (one located on the antenna axis and three located at various radial distances from the axis). For elements other than the central one of an array feed to compensate for losses due to a pointing error, they must contribute signal power in the direction of the pointing error. If a pointing error of 0.003 deg is assumed, from the figure it can be seen that only the first beam has any energy in that direction. The next beam ($Y = 1.8621$) is considerably more than 16 dB down from the contribution of the center element at 0.003 deg. (Note that the curves do not extend low enough to provide a more accurate value.) At this level the second element (or for that matter any of the other additional elements) cannot significantly contribute to improving the performance for a pointing error on the order of 0.003 deg. This effect can be seen for a 75-deg elevation angle in Fig. 12, where the separation of the four curves remains essentially constant as a function of boresight offset angle over typical pointing errors.

As will be seen later, significant pointing error improvements will not be seen until the feed size, and therefore the feed spacing, is reduced by three or more times and a larger number of elements is used. This problem is aggravated by the shaped reflector design of the 70-m antenna. Shaped designs provide nearly uniform illumination, which in turn provides the narrowest beamwidth for a given antenna size. Conventional antenna designs do not provide uniform illumination and therefore have much wider beamwidths. These wider beamwidths for conventional-design antennas allow higher crossovers between adjacent beams and therefore a higher potential to compensate for pointing errors than for shaped designs.

The following discussion applies to elevation angles of 75 deg. The hybrid-mode horn case (Fig. 12), over the range of -0.004 to 0.002 deg (for a pointing accuracy of 0.003 deg) with seven elements, gives an improvement over and above the distortion compensation of only 0.2 dB at -0.004 deg and 0.0 dB at 0.002 deg. Additional elements do not give any additional pointing-error compensation. The 1.75-in. dual-mode horn case (Fig. 14) has a performance very similar to the hybrid-mode horn case over the range of -0.004 to 0.002 deg, except for a 0.2-dB improvement at 0.002 deg for seven elements. Thus the larger horn sizes show little potential for pointing correction. The 1.25-in. dual-mode horn case (Fig. 15) shows improved pointing capability with additional elements over the same angles. Unfortunately, because of the lower performance at the best pointing angle, all the element curves for the 1.25-in. case are below the corresponding ones for the 1.75-in. case over a range of pointing errors of 0.006 deg. Therefore the 1.25-in. case is not as good a choice as the larger array sizes unless it is a requirement to support a range of pointing errors larger than 0.008 deg.

The arrays with smaller elements have much better pointing-error correction capability. The correction capability for the 0.35-in.-diameter single-mode horn is shown in Fig. 16. The performance with one or seven elements is not as good as can be achieved with 1.75-in. elements, since with such a small number of elements the antenna is overilluminated. The performance of the 0.35-in. case with 37 elements and no pointing correction falls between that for one element and that for seven elements for the 1.75-in. case. Over a range of pointing errors of 0.006 deg, the 0.35-in. case with 37 elements has from 1.0 to 1.2 dB better performance than the 1.75-in. case with seven elements and 0.8 and 0.9 dB better performance than the 1.75-in. case with 19 elements. The 0.35-in. case with 19 elements has 0.2 to 0.3 dB better performance than the 1.75-in. case with seven elements and no improvement over the 1.75-in. case with 19 elements. For error ranges greater than 0.006 deg, which could result from wind gusts, 0.35-in. arrays with 19 or more elements have

an advantage. This advantage, however, is at the expense of the better performance that would be achieved with 19 1.75-in. horns if the pointing errors were normally limited to a range of errors smaller than 0.006 deg.

For pointing error compensation and with 37-element designs, arrays with 0.35-in.-diameter horns are best. For 19-element designs, arrays with 0.35-in.-diameter horns are better when pointing errors are greater than ±0.003 deg. For seven-element designs, arrays with 1.75-in.-diameter horns are better, even though the 1.75-in. design has no pointing correction capability.

D. Performance Versus Subreflector Lateral Position

The ability of the array feed to improve performance was analyzed with the subreflector located at the position that gives the best performance as a function of elevation angle. In actual practice, the subreflector will normally be set at this location, and it is useful to know how accurately the subreflector needs to be positioned to maintain optimal performance. In addition, knowledge of the effect of array design on subreflector positional accuracy would be useful in the selection of an optimum array design. First consider the case using the hybrid-mode horn. Figure 17 shows the antenna at 45 deg, and therefore the results do not include any distortion effects. The number of elements has no effect on the performance until the positional errors exceed 0.1 in., well within the expected positional accuracy. In order to hold the losses within approximately 0.2 dB, the subreflector needs to be set within 0.03 in. Figure 18 shows the performance at an elevation angle of 75 deg. Although the performance is lower because of the surface distortions, the sensitivity to subreflector position for a single element remains about the same. Over the region of interest, additional elements do not improve performance. Figures 19 through 21 show the performance of the smaller feed elements. The 1.75-in. dual-mode design behaves essentially the same as the hybrid-mode design over the small range of displacements expected. The relative performance between elements of different sizes is similar to that seen for beam-pointing performance. The subreflector is less sensitive to position for the 1.25-in. dual-mode case than for the 1.75-in. case when the use of more than one element is considered. The 0.35-in. single-mode case has a low sensitivity to position with 19 elements, the minimum number of elements that is practical with elements of this size. With 37 elements, the 0.35-in. design is virtually insensitive to subreflector position over ±0.1 in. However, if the subreflector can be positioned within ±0.04 in., including wind gusts, then the seven-element 1.75-in. horn case still represents the best overall performance.

IV. Summary and Conclusions

The previous discussion covers the calculated performance of the 70-m antenna when used beyond its design frequency, where surface distortions detract from its performance. An array of circular feed horns arranged in a triangular lattice was used to recover some of the lost performance. A study was conducted to determine how effective this method is in recovering the lost performance so that the potential improvement from increasing the operating frequency can be judged.

Although the cost tradeoff for this concept is beyond the scope of this study, some useful observations can be made. It was indicated that the measured gain loss at 32 GHz at the rigging angle was 4.56 dB with a hybrid-mode feed horn. The calculated radio frequency (rf) losses, which do not include random small-scale surface distortions, quadripod blockage, or dissipation losses, for a single hybrid-mode horn with the antenna at the rigging angle are 0.37 dB. This indicates that the small-scale surface distortion, quadripod blockage, and dissipation losses are 4.19 dB. Adding this loss to the calculated rf loss of 3.48 dB at an elevation angle of 7.5 deg gives an overall loss of 7.67 dB. This is to be compared with a 1.8-dB loss at 8.4 GHz, composed of a 1.5-dB efficiency loss [2] and an antenna distortion loss of 0.3 dB at 7.5 deg. This gives a net loss of 5.87 dB at 32 GHz relative to 8.4 GHz at 7.5 deg. In order to evaluate the significance of this relative loss, this loss along with any relative losses associated with the spacecraft system would have to be subtracted from the potential gain increase of 11.6 dB due to frequency scaling. Thus, subtracting the 5.87-dB relative loss from 11.6 dB leaves a 5.73-dB net improvement, less any spacecraft-related losses.

As mentioned earlier, the small-scale rms error of the 70-m antennas is about 0.7 mm. A large part of this error is panel setting error. Recent data indicate that the panels could be readjusted, using holography techniques, to provide an rms error of about 0.45 mm. If this improvement can be achieved, 2.2 dB of the small-scale surface error losses could be recovered and as much as a 7.93-dB net improvement could be obtained. A long-term goal is to achieve a 0.25-mm rms surface accuracy by the year 2000, and this could provide 1.0 dB of additional improvement at 32 GHz.

As the study shows, some of the lost performance can be recovered with an array feed. It was further shown that arrays with 1.75-in.-diameter horns gave the best improvement for distortion errors. For seven elements at 7.5 deg, the array feed would recover 1.44 dB of the estimated 3.48-dB gravity distortion loss. Going to 19 or

37 elements would recover only an additional few tenths of a decibel and is not practical to consider at this time.

To provide pointing-error compensation, small array elements are required, with the 0.35-in.-diameter horn elements performing best. Although the peak gain of the 1.75-in. array elements in the boresight direction is higher than for the 0.35-in. elements, the scanning capabilities of a 37-element array of 0.35-in. elements allow it to exceed the static performance of an array of 1.75-in. elements. For pointing errors in excess of 0.003 deg, an array of 19 0.35-in. elements will give better performance. Using fewer than 19 elements for the 0.35-in. element array is not practical, since they would cover a smaller area than a single 1.75-in. horn. Since a single 1.75-in. horn is close to optimum for an undistorted antenna, a 0.35-in. array with fewer than 19 elements would never be able to effectively illuminate an undistorted antenna, much less a distorted one.

The question naturally arises as to why more of the energy lost to large-scale surface distortions cannot be recovered. Why is the recovery limited to about half of the lost power? There is no simple answer at this time. The analysis was done in the transmit mode. Patterns and excitations were assigned to the array feed, and the effect on the overall gain of the antenna was calculated in the presence of surface errors. This method gives no insight into what the focal fields look like and how they are affected by the antenna distortions. In addition, the transmit method gives no idea of how effectively the array feed system samples these focal plane fields. What is required is to calculate the performance in the receive mode. This would directly provide the focal plane fields. In turn, by correlating the aperture fields of the array horns with the focal plane fields, the performance of the antenna can be predicted. More importantly, greater visibility of what is happening to the fields in the focal plane region would provide a method for determining the best array geometry and horn type for surface-error compensation.

A program capable of efficiently computing the receive-mode patterns of a 70-m antenna at 32 GHz did not exist at the time this study began. Also the field correlation technique required needed to be developed. Further work needs to be done to implement and use the receive mode of analysis, and then other classes of feed horn designs need to be studied to determine how much more of the lost power can be recovered. If more of the lost power is recoverable, then it must be determined what the potential improvements are and whether array feeds represent the best way to implement a 32-GHz capability.

Acknowledgment

The author expresses appreciation to Dr. Roy Levy for supplying the mechanical model, along with the tables of gravity coefficients from which the distortion data required for this study were derived.

References

[1] M. S. Gatti, M. J. Klein, and T. B. H. Kuiper, "32-GHz Performance of the DSS-14 70-Meter Antenna; 1989 Configuration," *TDA Progress Report 42-99*, vol. July–September 1989, Jet Propulsion Laboratory, Pasadena, California, pp. 206–219, November 15, 1989.

[2] D. A. Bathker and S. D. Slobin, "DSN 70-Meter Antenna Microwave Optics Design and Performance Improvements; Part I: Design Optimization," *TDA Progress Report 42-97*, vol. January–March 1989, Jet Propulsion Laboratory, Pasadena, California, pp. 306–313, May 15, 1989.

[3] S. J. Blank and W. A. Imbriale, "Array Feed Synthesis for Correction of Reflector Distortion and Vernier Beamsteering," *IEEE Trans. Antennas Propagation*, vol. AP-36, no. 10, pp. 1351–1358, October 1988.

[4] R. Levy and R. Melosh, "Computer Design of Antenna Reflectors," *Journal of the Structural Division, ASCE*, vol. 99, no. ST11, Proc. Paper 10178, pp. 2269–2285, November 1973.

[5] V. Galindo-Israel, W. A. Imbriale, Y. Rahmat-Samii, and T. Veruttipong, "Interpolation Methods for Shaped Reflector Analysis," *IEEE Trans. Antennas Propagation*, vol. AP-36, no. 3, pp. 441–444, March 1988.

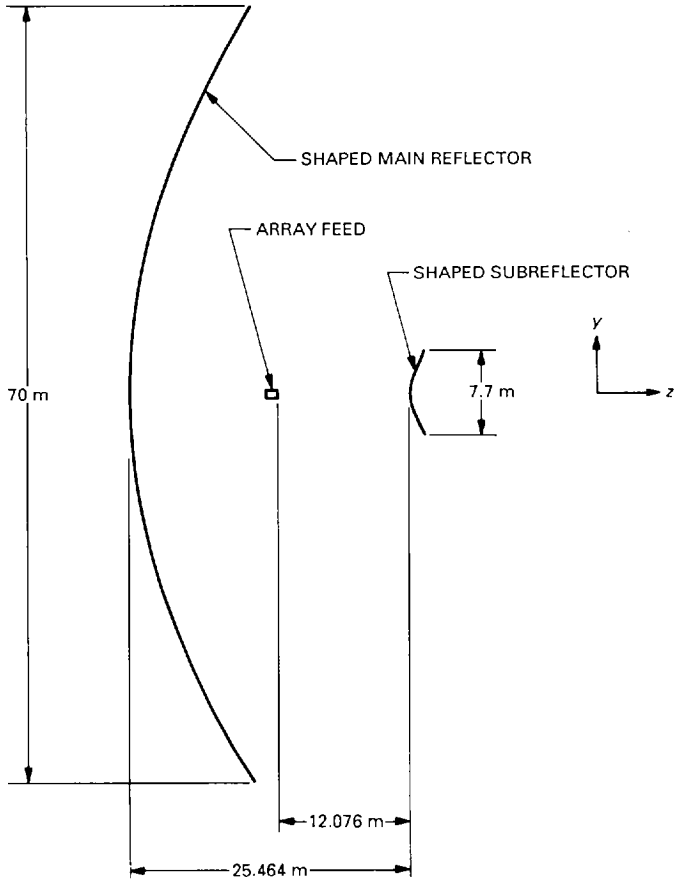

Fig. 1. Geometry of 70-m antenna.

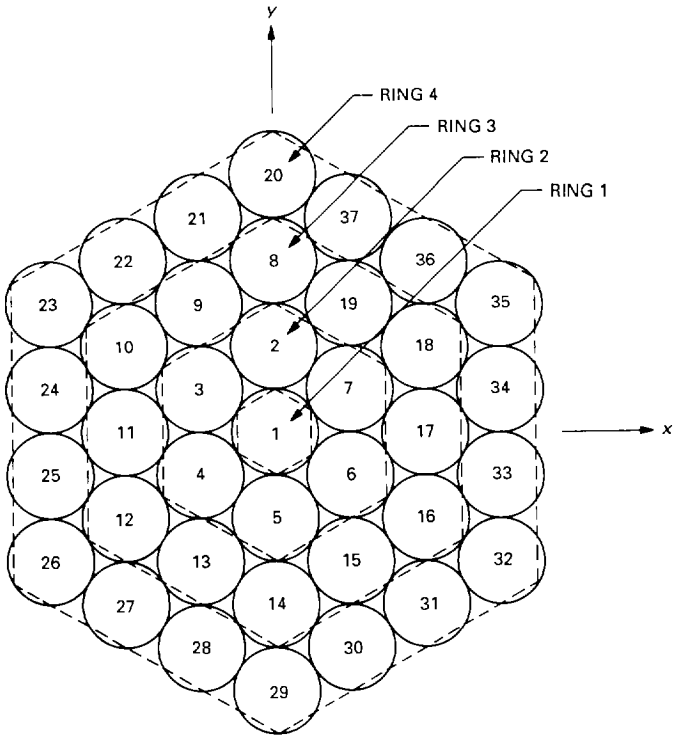

Fig. 2. Feed array configuration.

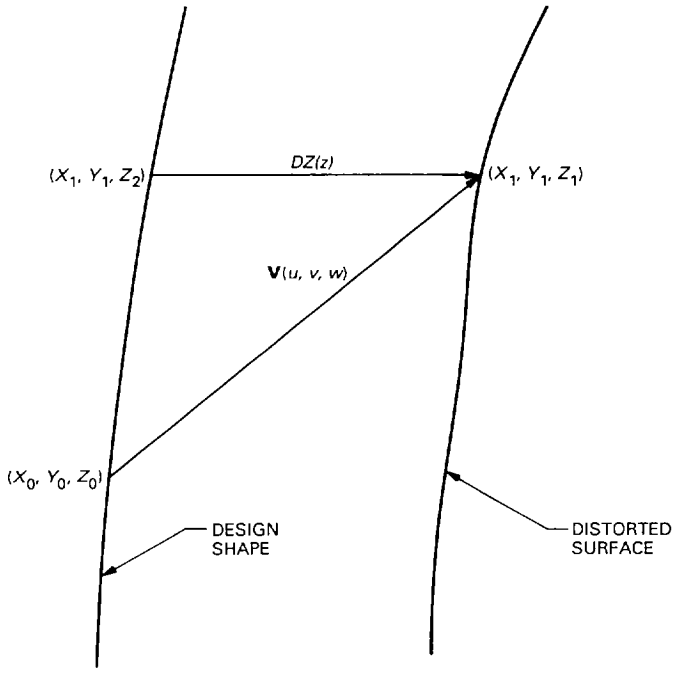

Fig. 3. Definition of surface distortion.

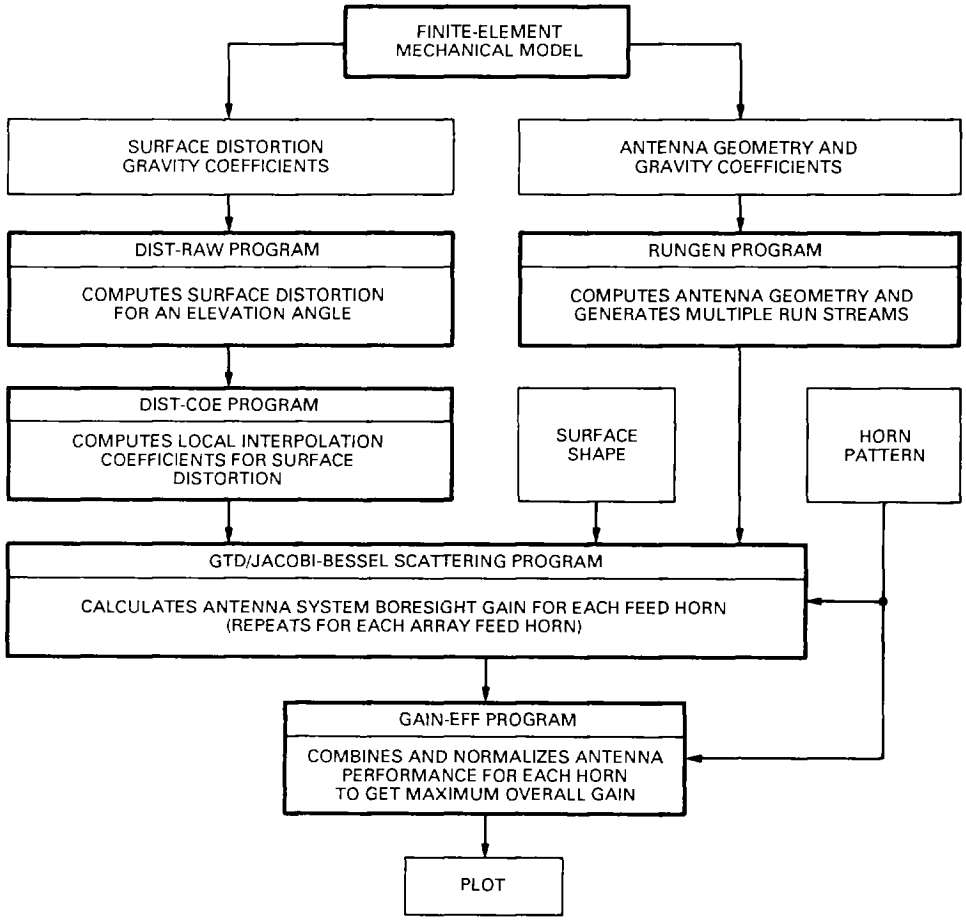

Fig. 4. Calculation flow diagram for analysis.

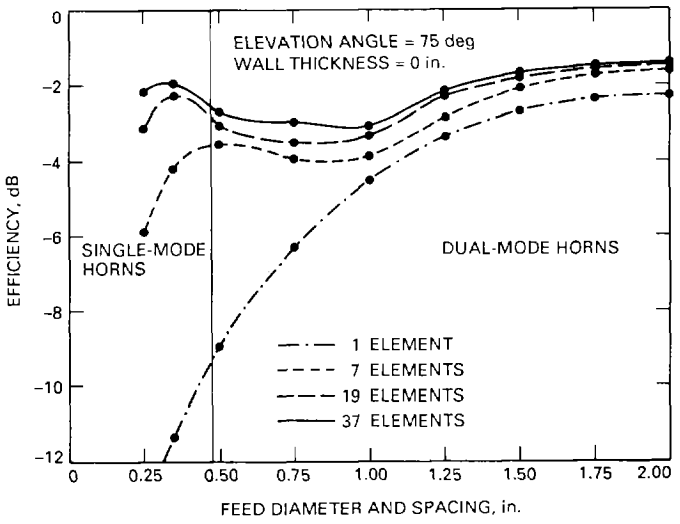

Fig. 5. Effect of feed element size on efficiency of 70-m antenna for arrays of elements with zero-thickness walls.

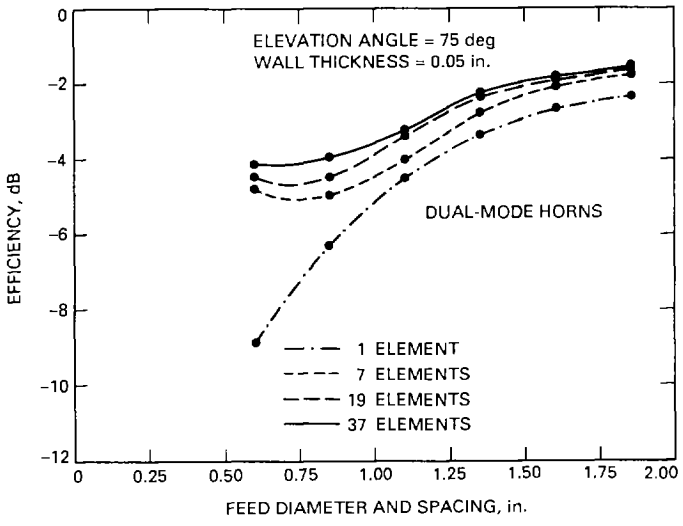

Fig. 6. Effect of feed element size on efficiency of 70-m antenna for arrays of elements with 0.05-in.-thick walls.

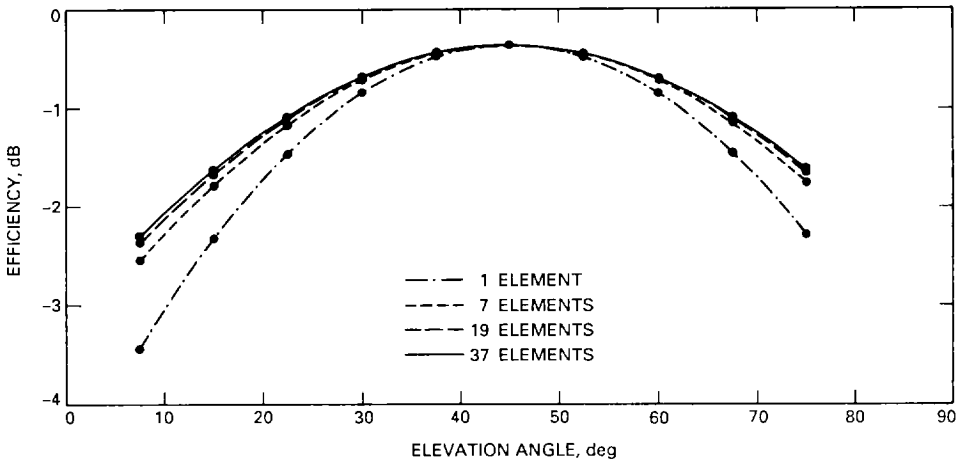

Fig. 7. Performance of 70-m antenna versus antenna elevation angle for arrays of 2.2-in.-diameter hybrid-mode feed horns.

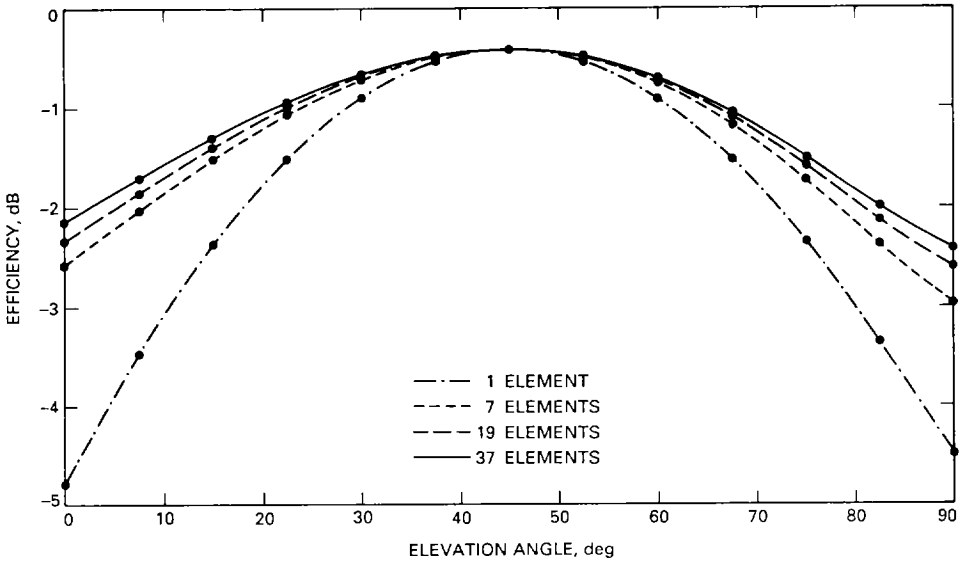

Fig. 8. Performance of 70-m antenna versus antenna elevation angle for arrays of 1.75-in.-diameter dual-mode feed horns.

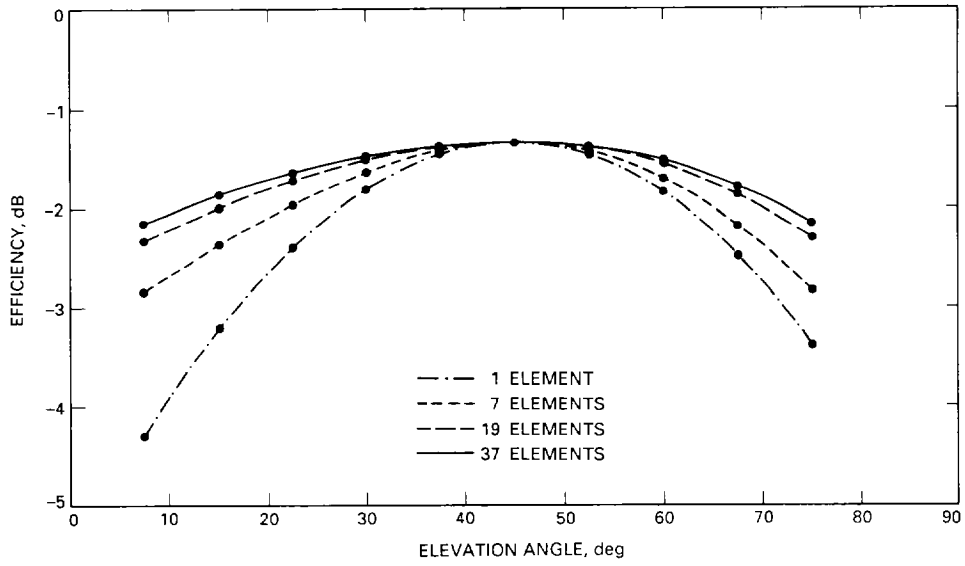

Fig. 9. Performance of 70-m antenna versus antenna elevation angle for arrays of 1.25-in.-diameter dual-mode feed horns.

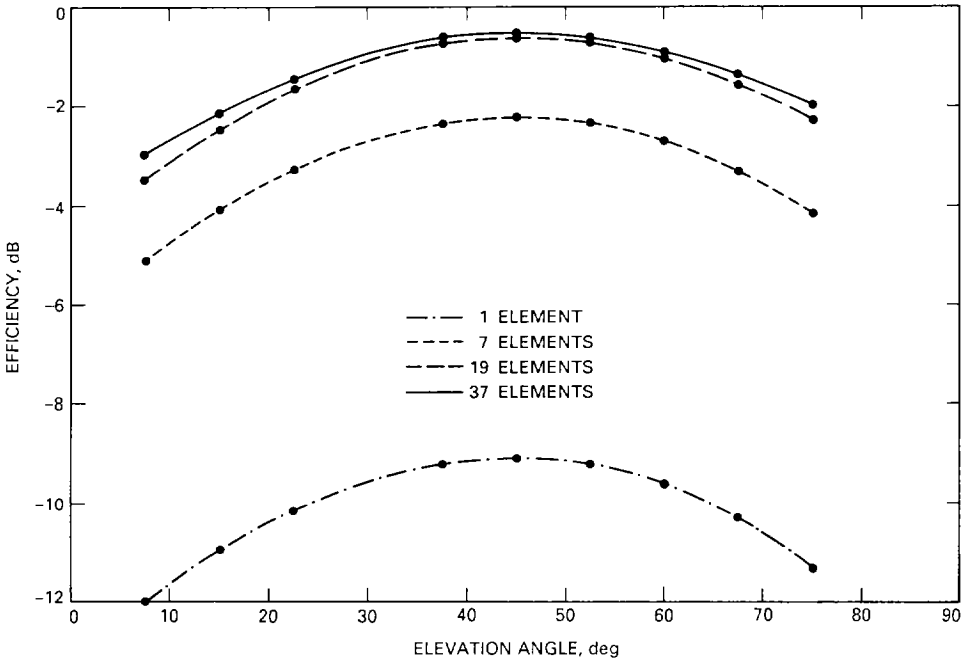

Fig. 10. Performance of 70-m antenna versus antenna elevation angle for arrays of 0.35-in.-diameter single-mode feed horns.

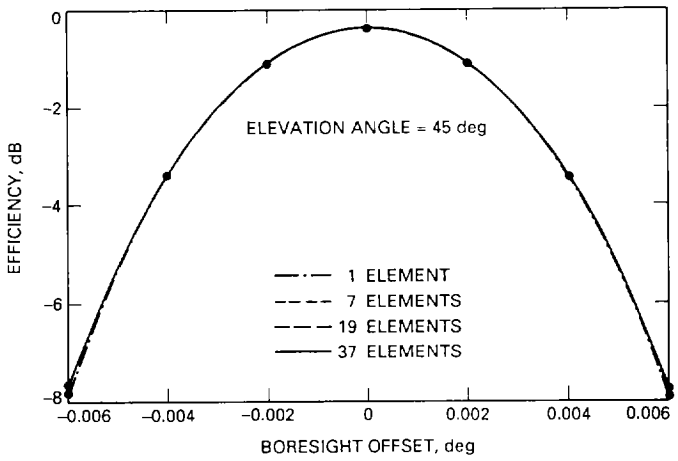

Fig. 11. Effect of antenna pointing error on performance of 70-m antenna for arrays of 2.2-in.-diameter hybrid-mode feed horns at 45 deg.

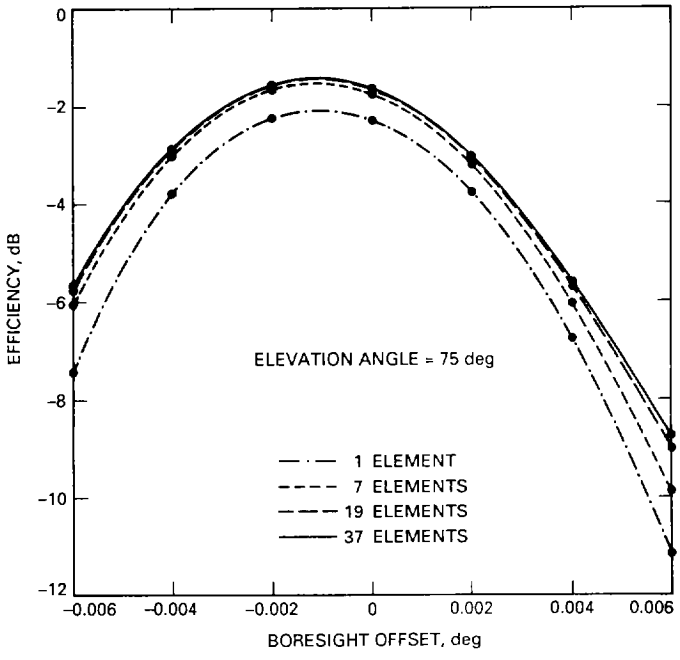

Fig. 12. Effect of antenna pointing error on performance of 70-m antenna for arrays of 2.2-in.-diameter hybrid-mode feed horns at 75 deg.

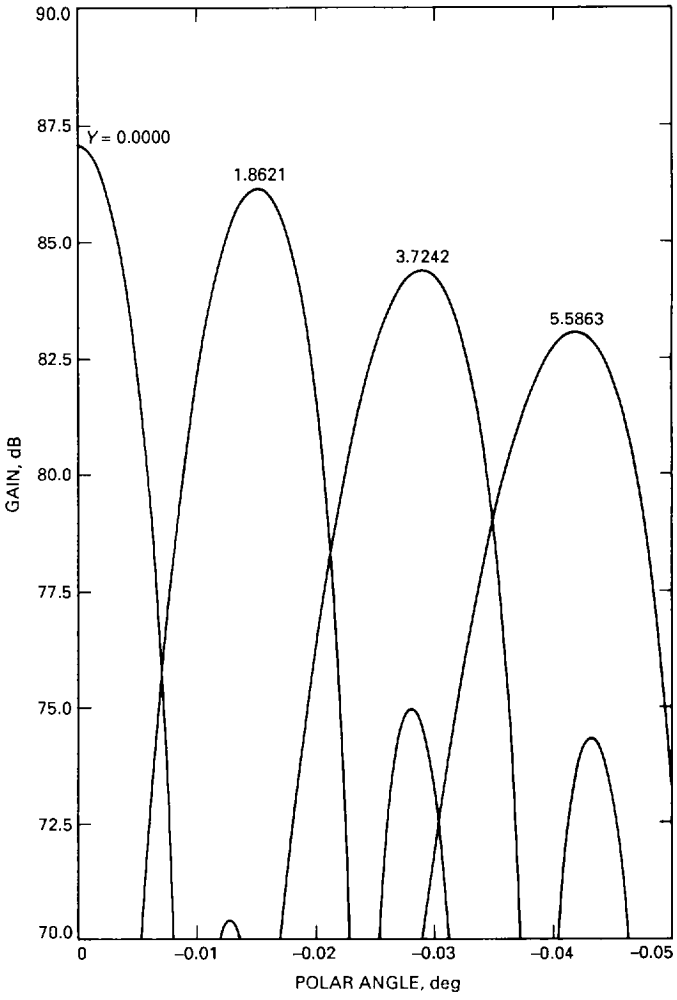

Fig. 13. Beam patterns of 70-m antenna for hybrid-mode feed horns at four different lateral offset positions.

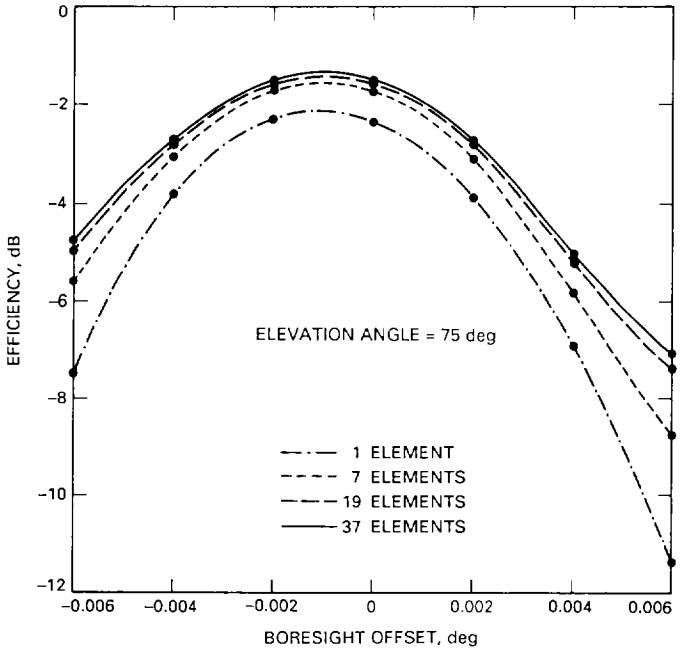

Fig. 14. Effect of antenna pointing error on performance of 70-m antenna for arrays of 1.75-in.-diameter dual-mode feed horns.

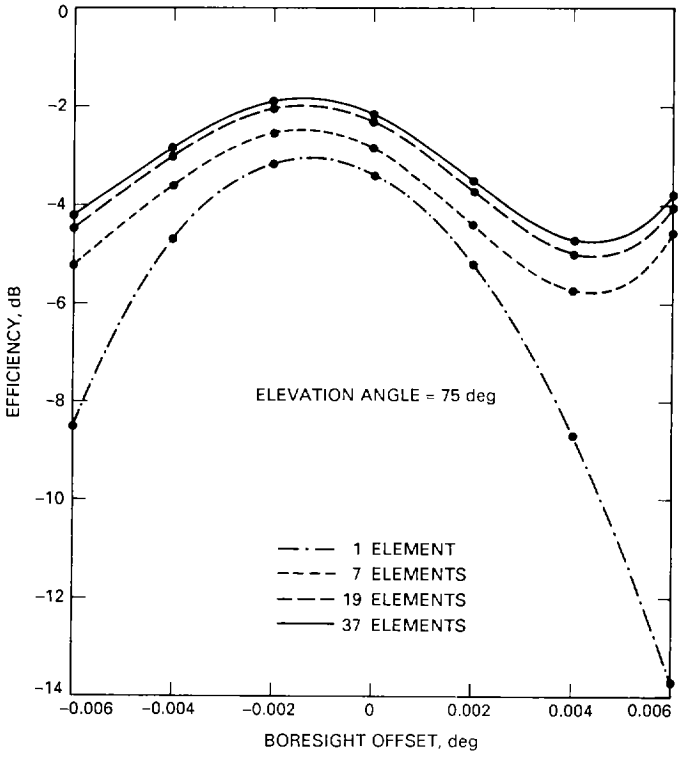

Fig. 15. Effect of antenna pointing error on performance of 70-m antenna for arrays of 1.25-in.-diameter dual-mode feed horns.

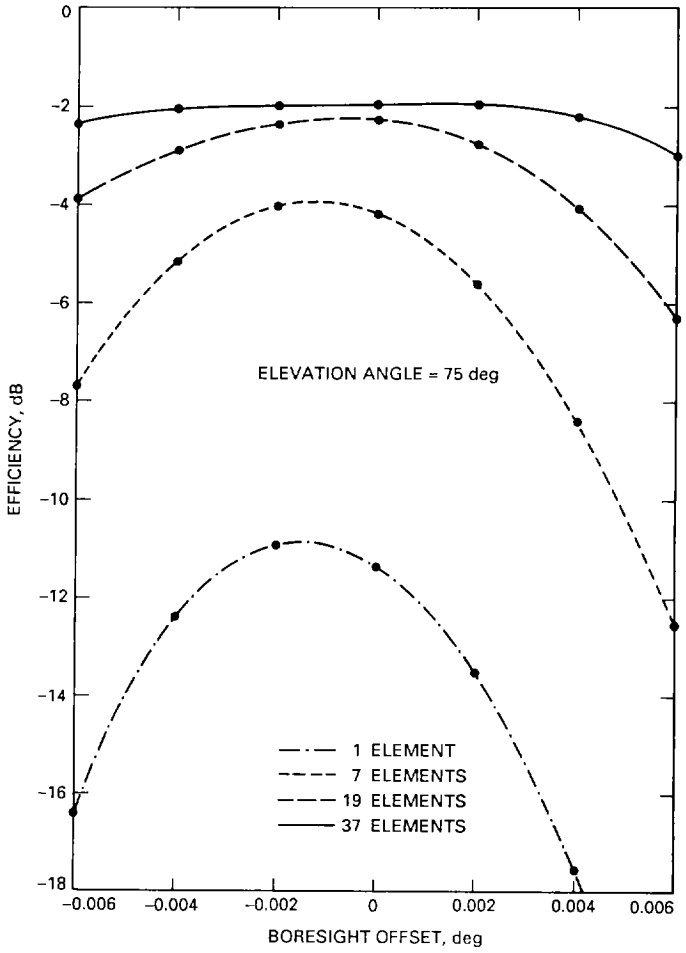

Fig. 16. Effect of antenna pointing error on performance of 70-m antenna for arrays of 0.35-in.-diameter single-mode feed horns.

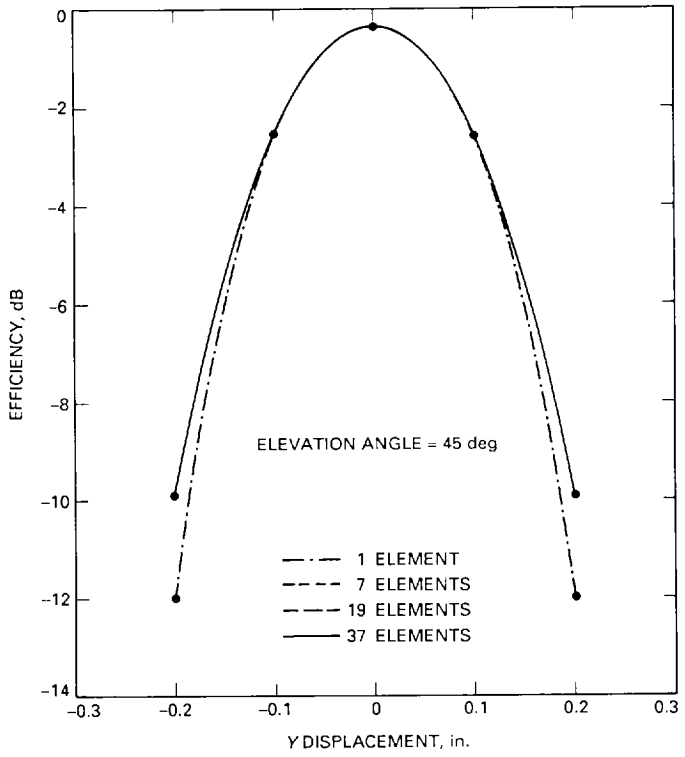

Fig. 17. Effect of subreflector displacement on performance of 70-m antenna for arrays of 2.2-in.-diameter hybrid-mode feed horns at 45 deg.

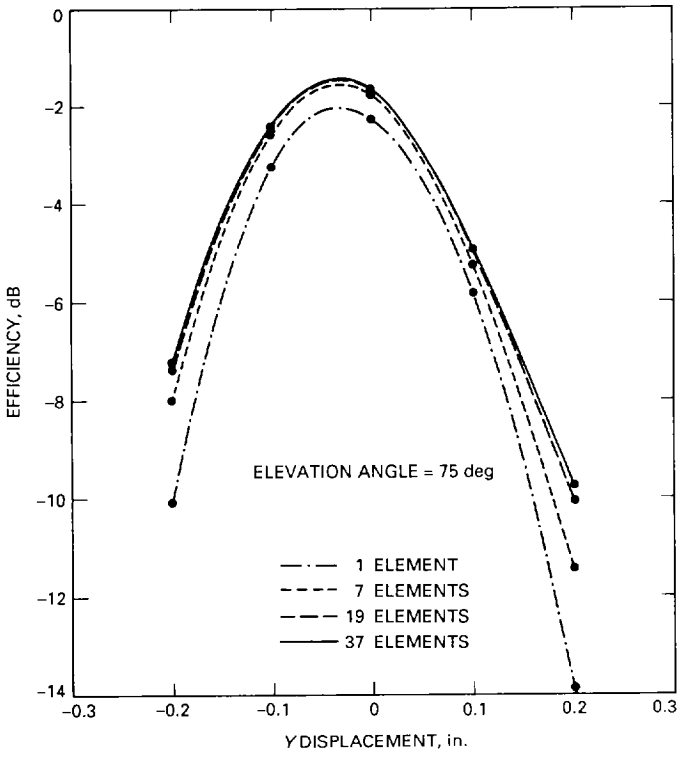

Fig. 18. Effect of subreflector displacement on performance of 70-m antenna for arrays of 2.2-in.-diameter hybrid-mode feed horns at 75 deg.

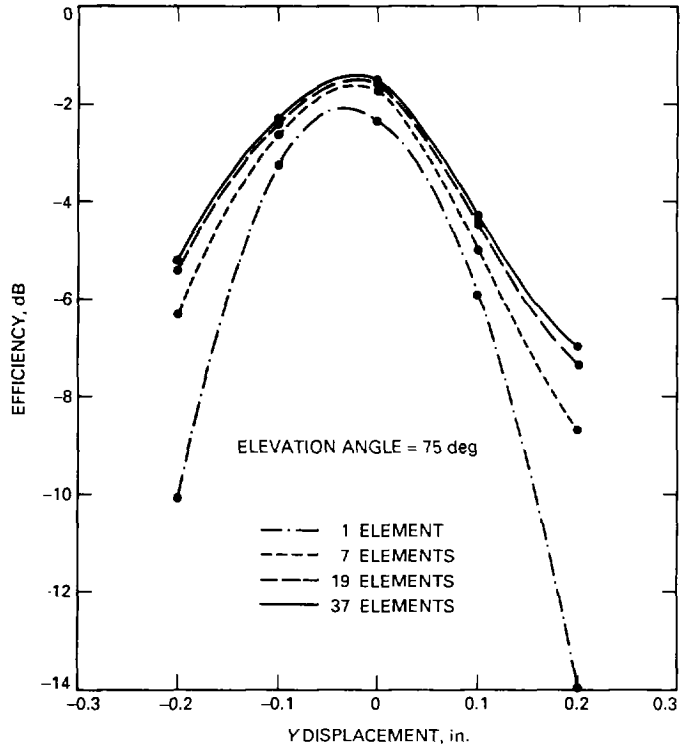

Fig. 19. Effect of subreflector displacement on performance of 70-m antenna for arrays of 1.75-in.-diameter dual-mode horns.

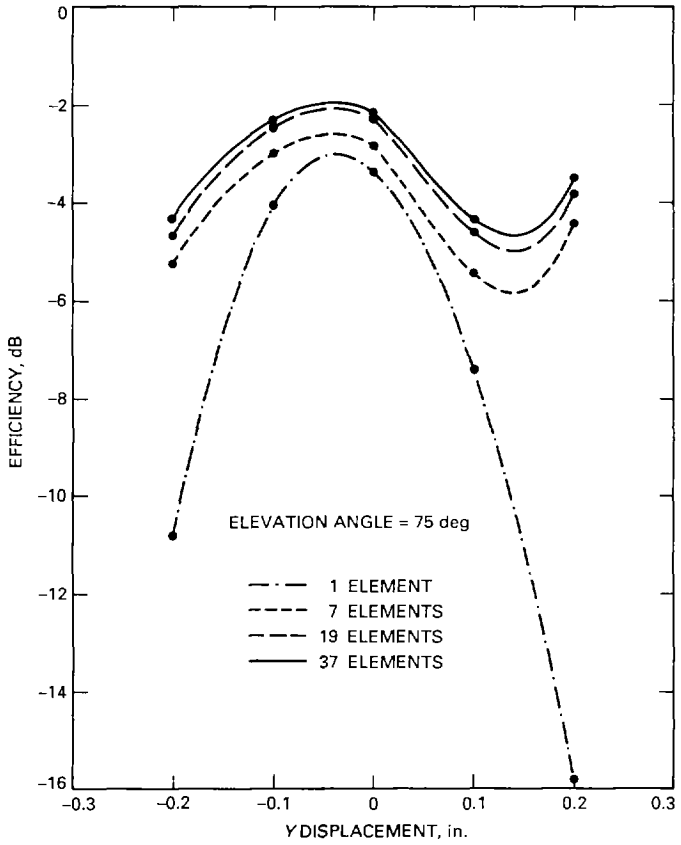

Fig. 20. Effect of subreflector displacement on performance of 70-m antenna for arrays of 1.25-in.-diameter dual-mode horns.

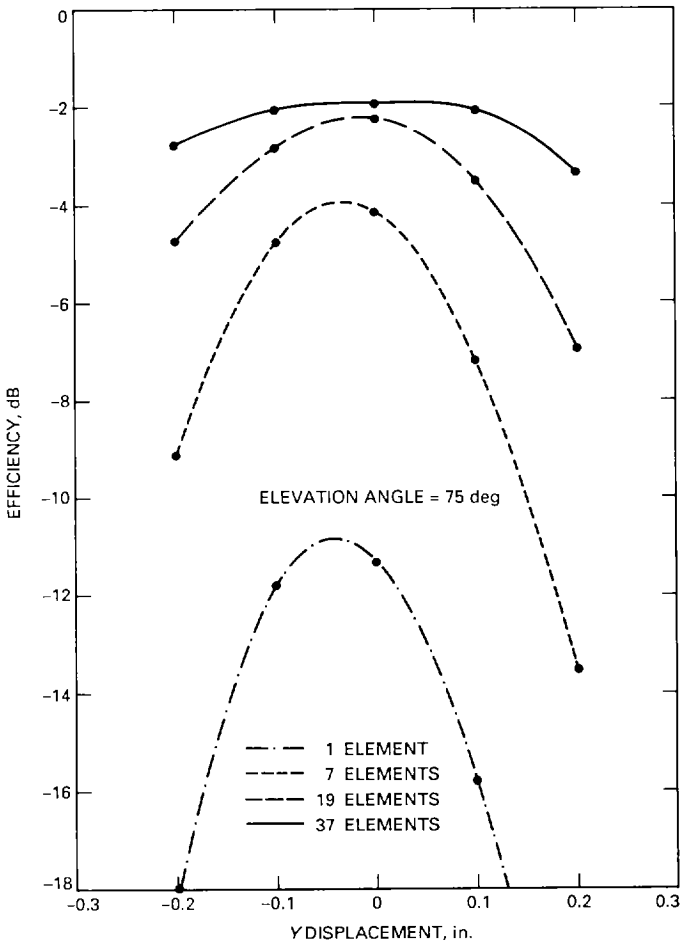

Fig. 21. Effect of subreflector displacement on performance of 70-m antenna for arrays fo 0.35-in.-diameter single-mode horns.